Complexation of daclatasvir by single isomer methylated β-cyclodextrins studied by capillary electrophoresis, NMR spectroscopy and mass spectrometry

Sulaiman Krait[a], Antonio Salgado[b], Paola Peluso[c], Milo Malanga[d], Tamas Sohajda[d], Gábor Benkovics[d], Lukas Naumann[e], Christian Neusüß[e], Bezhan Chankvetadze[f], Gerhard K. E. Scriba[a,*]

[a] Friedrich-Schiller-University Jena, Department of Pharmaceutical/Medicinal Chemistry, Philosophenweg 14, 07743 Jena, Germany

[b] University of Alcalá, NMR Spectroscopy Centre (CERMN), CAI Químicas, Faculty of Pharmacy, 28805 Alcalá de Henares, Madrid, Spain

[c] Istituto di Chimica Biomolecolare, Consiglio Nazionale delle Ricerche, Traversa La Crucca, 3 - Regione Baldinca - Li Punti, 07100 Sassari, Italy

[d] CycloLab Ltd., Illatos út 7, 1097 Budapest, Hungary

[e] Aalen University, Department of Chemistry, Beethovenstrasse 1, 73430 Aalen, Germany

[f] Tbilisi State University, Institute of Physical and Analytical Chemistry, School of Exact and Natural Sciences, 0179 Tbilisi, Georgia

Correspondence:
Prof. Dr. Gerhard K. E. Scriba
Friedrich Schiller University Jena,
Department of Pharmaceutical/Medicinal Chemistry
Philosophenweg 14
07743 Jena, Germany
Phone: +49-3641-949830
E-Mail: gerhard.scriba@uni-jena.de

Abstract

In capillary electrophoresis an enantioseparation of daclatasvir (DCV) was observed in case of heptakis(2,6-di-*O*-methyl)-β-CD, heptakis(2-*O*-methyl)-β-CD and β-CD, while two peaks with a plateau were noted for heptakis(2,3,6-tri-*O*-methyl)-β-CD and heptakis(2,3-di-*O*-methyl)-β-CD indicating a slow equilibrium. Heptakis(6-*O*-methyl)-β-CD and heptakis(3-*O*-methyl)-β-CD yielded broad peaks. Nuclear magnetic resonance experiments including nuclear Overhauser effect-based techniques revealed inclusion complex formation for all CDs with the biphenyl ring of DCV within the cavity and the valine-pyrrolidine moieties protruding from the torus. However, in case of heptakis(2,6-di-*O*-methyl)-β-CD, heptakis(2-*O*-methyl)-β-CD and β-CD higher order structures with 1:3 stoichiometry were concluded, where the valine moieties enter additional CD molecules via the secondary side. Heptakis(2,3,6-tri-*O*-methyl)-β-CD and heptakis(2,3-di-*O*-methyl)-β-CD yielded primarily 1:1 complexes. Higher order complexes between DCV and heptakis(2,6-di-*O*-methyl)-β-CD were corroborated by mass spectrometry. Complex stoichiometry was not the reason for the slow equilibrium yielding the plateau observed in capillary electrophoresis, but structural characteristics of the CDs especially complete methylation of the secondary rim.

Keywords: Cyclodextrin-analyte complexation; Complex stoichiometry; Complex structure; Capillary electrophoresis; Nuclear magnetic resonance; Mass spectrometry

1 Introduction

Daclatasvir (DCV, dimethyl N,N'-([1,1'-biphenyl]-4,4'-diylbis{1H-imidazole-4,2-diyl-[(2S)-pyrrolidine-2,1-diyl][(2S)-3-methyl-1-oxobutane-1,2-diyl]})dicarbamate, Figure 1) is an inhibitor of the hepatitis C nonstructural protein 5A replication complex (Belema et al., 2014). The drug is used in combination with sofosbuvir for the treatment of infections with hepatitis C virus genotypes 1 – 4 (Pawlotsky et al., 2018). DCV is a "symmetrical" biphenyl with two identical halves consisting of an imidazole-pyrrolidine-*N*-methoxycarbonyl-valine moiety containing two stereogenic centers. The pharmacological active stereoisomer possesses *S*,*S*,*S*,*S* configuration. Apart from the *R,R,R,R*-configured enantiomer (*RRRR*-DCV, Figure 1) further diastereomers including meso forms exist.

Capillary electrophoresis (CE) is considered a high-resolution technique for stereoisomer separations of polar and ionogenic analytes (Bernardo-Bermejo, Sanchéz-López, Castro-Puyana, & Marina 2020; Fanali, & Chankvetadze, 2019; Chankvetadze, 2018; Jáč, & Scriba, 2013). Enantioseparations are based on the formation of transient diastereomeric complexes between the enantiomers and a chiral selector added to the background electrolyte (BGE). With regard to chiral selectors, cyclodextrins (CDs) are by far the most often applied selectors for enantioseparations in CE (Zhu, & Scriba, 2016; Yu, & Quiriino, 2019; Fejös, Kalydi, Malanga, Benkovics, & Beni, 2020; Guo, & Xiao, 2021). In order to rationalize the complexation between analytes and CDs and, consequently, the chiral recognition of the selector, the structures of the complexes have been analyzed by NMR spectroscopy (Chankvetadze, 2004; Dodziuk, Koźmiński, & Ejchart 2004; Salgado & Chankvetadze, 2016; Silva, 2017). Techniques such as rotating frame nuclear Overhauser enhancement spectroscopy (ROESY) are useful as these methods point out hydrogen atoms that are spatially close. NMR experiments with CDs as water soluble selectors can be conducted under basically identical conditions as those used in CE experiments.

When studying the enantioseparation of DCV by CE using CDs as chiral selectors, it was recently noted that an enantioseparation was achieved using randomly methylated β-CD, while two peaks with a plateau in between were observed in the presence of γ-CD, which represented a slow equilibrium between DCV-γ-CD complexes and non-complexed DCV (Krait et al., 2020). In addition, an unexpected observation in this study was the faster migration of the complex compared to free DCV. Apart from randomly methylated β-CD, the single isomer CDs heptakis(2,6-di-*O*-methyl)-β-CD (2,6-DM-β-CD) and heptakis(2,3,6-tri-*O*-methyl-β-CD (TM-β-CD) (Figure 1) have been commercially available for a long time. Recently, the synthesis and analytical application of further single isomer methylated β-CDs, i.e, heptakis(2-*O*-methyl)-β-CD (2-M-β-CD), heptakis(3-*O*-methyl)-β-CD (3-M-β-CD), heptakis(6-O-methyl)-β-CD (6-M-β-CD) and heptakis(2,3-di-*O*-methyl)-β-CD (2,3-DM-β-CD) (Figure 1) has been described (Varga et al., 2019). Heptakis(3,6-di-*O*-methyl)-β-CD was also synthesized but the poor aqueous solubility of less than 0.1 mg/mL prevented the application of this CD in CE using aqueous BGEs (Varga et al., 2019). Thus, the aim of the present study was the investigation of the separation of DCV and the enantiomer *RRRR*-DCV by single isomer methylated β-CDs and the determination of the DCV-CD complexes by NMR spectroscopy and mass spectrometry. Native β-CD was included for comparison. The hypothesis was whether the separation behavior observed in CE would be reflected in structural differences of the DCV–CD complexes. A second aspect was the migration sequence complex versus free analyte.

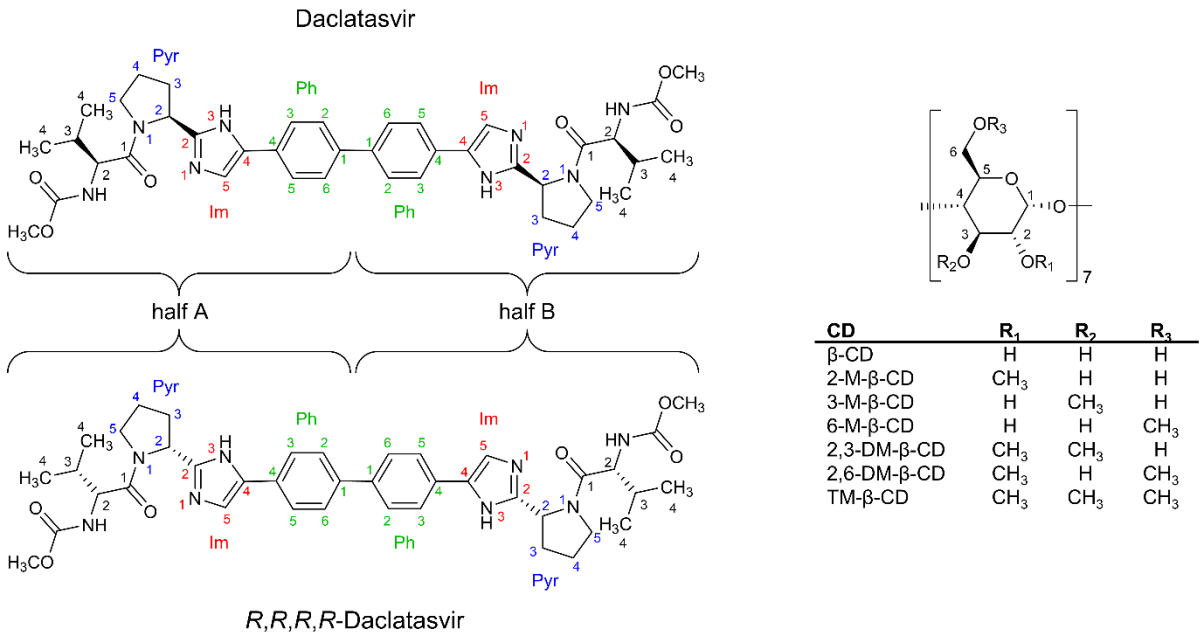

CD	R_1	R_2	R_3
β-CD	H	H	H
2-M-β-CD	CH_3	H	H
3-M-β-CD	H	CH_3	H
6-M-β-CD	H	H	CH_3
2,3-DM-β-CD	CH_3	CH_3	H
2,6-DM-β-CD	CH_3	H	CH_3
TM-β-CD	CH_3	CH_3	CH_3

Figure 1 Structures of daclatasvir (DCV), the *R*,*R*,*R*,*R*-enantiomer and methylated β-CDs. The numbers and labels refer to the description of the respective moieties in the text.

2 Materials and Methods

2.1. Chemicals

DCV dihydrochloride was a gift from Mylan Laboratories Ltd. (Hyderabad, India), while *RRRR*-DCV dihydrochloride was kindly supplied by Laurus Labs Ltd. (Hyderabad, India). β-CD, 2-M-β-CD, 3-M-β-CD, 6-M-β-CD, 2,3-DM-β-CD, 2,6-DM-β-CD and TM-β-CD were supplied by CycloLab (Budapest, Hungary). All other chemicals were of analytical grade and obtained from commercial sources. Water was purified using a TKA Genpure UV-TOC from Thermo Scientific (Waltham, MA, USA). BGEs and sample solutions were filtered through 0.22 µm polypropylene syringe filters from BGB Analytik (Schloßböckelheim, Germany).

2.2. Capillary electrophoresis

CE experiments were carried out on a Beckman P/ACE MDQ capillary electrophoresis system (Beckman Coulter, Krefeld, Germany) equipped with a UV-Vis diode array detector and controlled by the 32 KARAT software (version 8.0) for system control, data acquisition and processing. 40/50.2 cm, 50 µm i.d., 365 µm o.d. fused-silica capillaries were from CM Scientific (Silsden, UK). A new capillary was rinsed at a pressure of 20 psi (138 kPa) with 1 M NaOH for 20 min, followed by water for 10 min. Before each run, the capillary was flushed with water for 2 min followed by the BGE for 2 min. Experiments were carried out at 20 °C and an applied voltage of 25 kV. The detection wavelength was 305 nm. Samples were injected hydrodynamically at a pressure of 0.7 psi (4.8 kPa) for 5 s. 50 mM BGEs were prepared on a daily basis by dilution of 1 M phosphoric acid to approx. 80% of the final volume. The CD was added, and the pH was adjusted with 1 M NaOH before making up to the final volume. BGEs were degassed by sonication before use.

2.3. NMR spectroscopy

NMR spectra were recorded on a Varian NMR System (Varian Inc, Palo Alto, CA, USA), equipped with a CHX $^{1}H/^{13}C/^{15}N$-^{31}P probe head, a gradient module and a variable temperature unit. The resonance frequency for ^{1}H was 499.61 MHz. The 90º hard pulse for proton was optimized for each sample. The signal of residual HDO (4.65 ppm) served as internal standard. ^{1}H signals were assigned upon correlation spectroscopy (COSY), heteronuclear single quantum coherence (HSQC) and 1D total correlation spectroscopy (TOCSY) results when appropriate. COSY, HSQC and ROESY experiments were run with presaturation of the water signal. For the 1D TOCSY experiments, the spinlock (mixing) time was set to 80 ms. The structures of the supramolecular complexes were derived from 1D and 2D ROESY spectra at 400 ms mixing time. NMR data were processed with the MestReNova software (v. 14.2.0, Mestrelab Research, S.L., Santiago de Compostela, Spain). Samples were prepared by weighing about 12 to 17 mg of the respective CD and/or 2 to 3 mg of DCV or *RRRR*-DCV and dissolving in 0.6 to 0.8 mL of 50 mM D_3PO_3 in D_2O adjusted to an apparent pH 2.5 with NaOD.

2.4. Mass spectrometry

Electrospray ionization-mass spectrometry (ESI-MS) experiments were carried out on a Bruker Compact QTOF with an ESI Source (Bruker Daltonics, Bremen, Germany) using direct infusion. The sample was delivered by a syringe pump Model 100 Series (KD Scientific, Holliston MA, U.S.A.) with a 500 µL syringe (Trajan Scientific, Victoria, Australia) at a sample delivery flow rate of 4 µL/min. The instrument settings were as follows: nebulizer pressure of 0.3 bar, dry gas flow of 3 L/min at a temperature of 200 °C, capillary voltage 3,8 kV, end plate offset 500 V. Measurements were performed in a m/z-range of 200-5000 and with an acquisition rate of one spectrum per second. The sample contained 0.2 µM of the CD and 0.1 µM of DCV in a 100 mM ammonium formate buffer adjusted to pH 2.6 by addition of 2% ammonia solution.

3 Results and discussion

3.1 Capillary electrophoresis

The separation of DCV and the enantiomer *RRRR*-DCV was studied in 50 mM sodium phosphate buffer, pH 2.5, in the presence of native β-CD and single isomer methylated β-CDs. Because the limiting aqueous solubility of 2-M-β-CD and 6-M-β-CD at 25 °C is about 8 mM (10 mg/mL) (Varga et al., 2019), the enantioseparation of DCV by methylated β-CDs was studied at a concentration of 7 mM. The results are shown in Figure 2. The CDs can be divided into 3 groups. (1) Enantioseparations occurred in the presence of 2,6-DM-β-CD and 2-M-β-CD, (2) a single broad or a tailing peak in case of 3-M-β-CD and 6-M-β-CD and (3) two peaks with a plateau in between using 2,3-DM-β-CD or TM-β-CD. In the presence of 2,3-DM-β-CD and TM-β-CD, two peaks with a plateau were also obtained when enantiopure DCV or *RRRR*-DCV were analyzed (data not shown) so that the two peaks do not represent enantiomers. Although much higher concentrations were required, β-CD also yielded an enantioseparation albeit with opposite enantiomer migration order (EMO) compared. Thus, the substitution pattern of the CDs affected the general outcome of the CE analysis. Methylation of both positions 2 and 3 resulted in the plateau phenomenon, while an enantioseparation is observed in case of a methyl group in position 2.

However, the EMO is opposite to β-CD indicating different chiral recognition by native β-CD and methylated CDs. Methylation of positions 3 or 6 alone did not yield chiral separations.

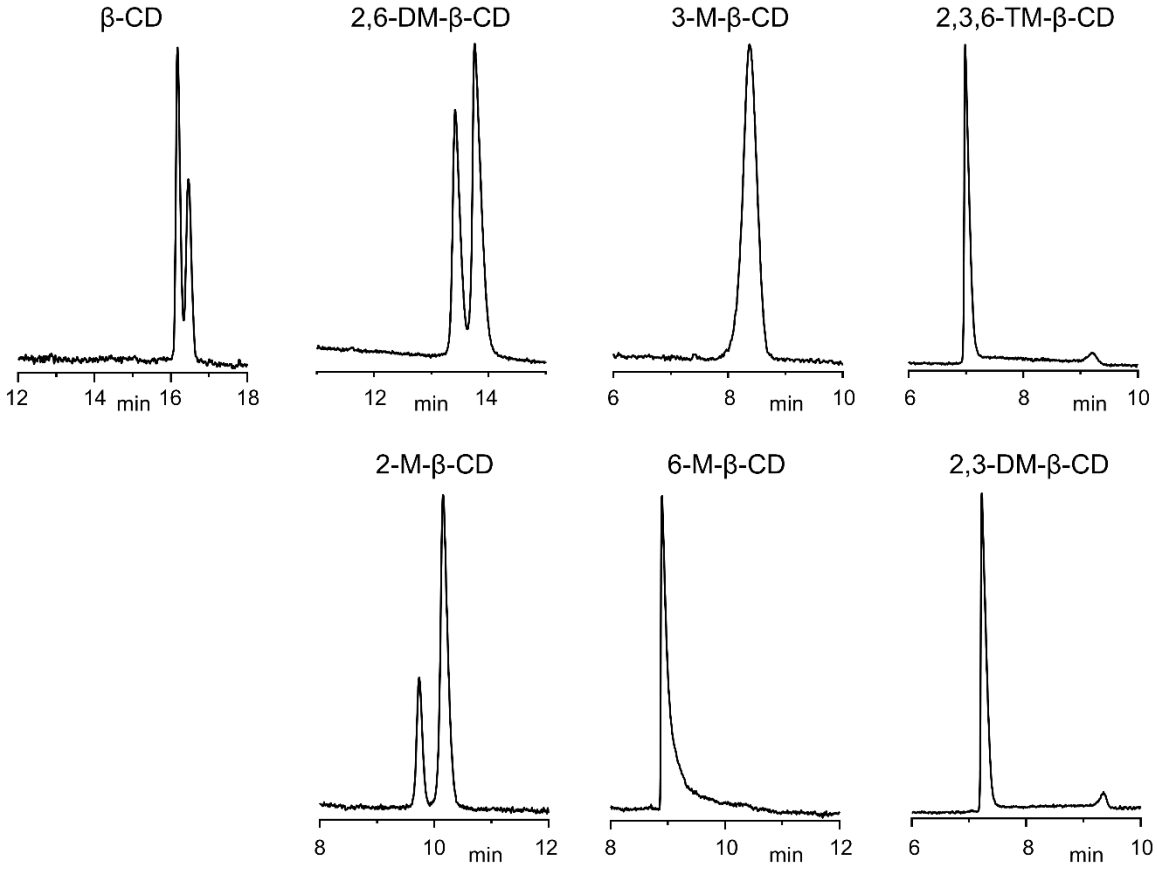

Figure 2 Electropherograms of the CE separation of a non-racemic mixture of DCV and *RRRR*-DCV (ratio about 2:1) in the presence of the indicated CDs. Experimental conditions: 40/50.2 cm, 50 µm id fused-silica capillary; 50 mM sodium phosphate buffer, pH 2.5; 20 °C; 25 kV; CD concentrations: 7 mM except β-CD 60 mM. The BGE containing β-CD also contained 5 M urea.

Due to the limited available quantities of most single isomer CDs, the effect of the concentration of the CDs could not be studied except for 2,6-DM-β-CD and TM-β-CD. In case of 2,6-DM-β-CD, increasing concentrations resulted in a deterioration of the enantioseparation so that only a shoulder was visible at a concentration of 20 mM (data not shown). In contrast, 20 mM TM-β-CD did not alter the general appearance of the electropherogram compared to 7 mM with the exception that the height of the plateau increased with the CD concentration. Interestingly, a plateau also resulted when a sample containing premixed DCV and TM-β-CD was analyzed using a CD-free BGE. Similar observations have been made previously for the analysis of DCV in the presence of γ-CD (Krait et al., 2020). Under these conditions, the two peaks with the plateau represented the slow equilibrium between γ-CD–DCV complexes and free, non-complexed DCV. Interestingly, these complexes migrated faster than the free analyte. In order to determine the migration order in case of TM-β-CD, individual plugs of DCV and TM-β-CD or a premixed sample containing both compounds were injected into a capillary containing CD-free BGE. The plugs were separated by a small plug of BGE in order to avoid mixing by diffusion in the capillary

before application of the voltage. The results are shown in Figure 3. When DCV was injected as the first plug, so that the compound did not migrate through the TM-β-CD plug on its way to the detector, only a single peak was observed at the migration time of DCV (Figure 3A). Reversing the injection order, so that DCV had to migrate through the CD plug, yielded two peaks with a flat plateau in between (Figure 3B). Injection of premixed DCV and TM-β-CD resulted also in two peaks as mentioned above. However, in this case the peak area of the second migrating peak was larger than the first migrating peak in contrast to the situation when DCV was analyzed with TM-β-CD containing BGEs (Figure 2). The area of the first migrating peak increased significantly, when a DCV plug was placed before the plug containing the mixture of DCV and TM-β-CD (Figure 3D) suggesting that the first peak is DCV while the second peak appears to be the DCV-CD complex(es). Thus, the migration order of free analyte and complexes is in the expected sequence with the smaller analyte migrating first based on the higher charge-to-mass ratio.

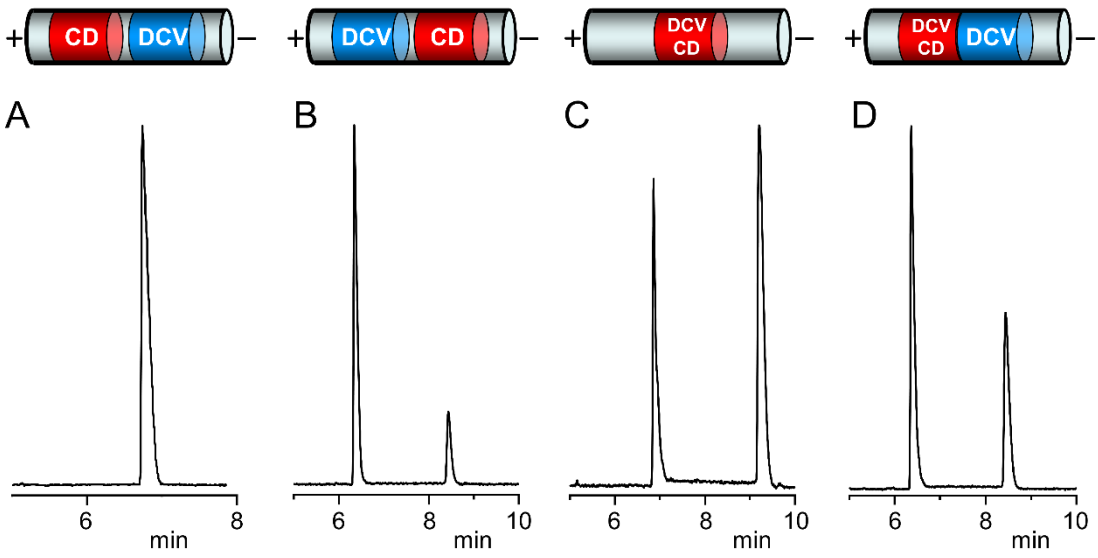

Figure 3 Pug-plug CE experiments for the determination of the migration sequence. The order of the injection of the plugs is schematically shown above the electropherograms. Injection sequence (A) DCV > TM-β-CD, (B) TM-β-CD > DCV, (C) DCV + TM-β-CD and (D) DCV > DCV + TM-β-CD. The concentration of the DCV sample was 200 µg/mL and the concentration of TM-β-CD was 20 mM (28.6 mg/mL). Experimental conditions as in Figure 2.

Assuming that the plateau represented the equilibrium between free and complexed analyte, which is slow in the CE timescale as in case of γ-CD (Krait et al., 2020), the capillary temperature was varied between 20 and 50 °C (Figure S1). The data hinted at a dynamic equilibrium in the capillary. At lower temperatures the exchange regime is slow and accelerates at higher temperatures. Thus, a more pronounced plateau is initially observed with increasing temperature, eventually resulting in coalescence at about 45 °C. A similar behavior was reported previously for γ-CD and DCV (Krait et al., 2020).

3.2. NMR

The structures of the complexes of DCV with the single isomer methylated β-CDs as well as native β-CD in solution were studied by ^{1}H NMR spectroscopy in deuterated sodium phosphate buffer using nuclear Overhauser effect (NOE) based methods, which allow the analysis of spatially close protons. In case of DM-β-CD and TM-β-CD, the complexes with the *RRRR*-DCV enantiomer were also analyzed. Signals were assigned using COSY, TOCSY and HSQC data.

3.2.1 Complex DCV and 2,6-DM-β-CD

The ^{1}H-NMR spectra of 2,6-DM-β-CD, DCV and a mixture of DCV and 2,6-DM-β-CD are shown in Figure 4. The spectra of the CD (Figure 4A) and the DCV (Figure 4B) are in accordance with earlier reported spectra for 2,6-DM-β-CD (Varga et al., 2019) and DCV, for a detailed discussion of the solution structure of DCV see (Krait et al., 2020). The spectrum of the mixture (Figure 4C) looked well resolved, with quite sharp signals, yet with some overlapping. Signal assignments of the mixture are summarized in Table S1 (supplementary material). A total of five sets of signals were observed upon close inspection. Two of these sets are consistent with the 2,6-DM-β-CD structure, for instance the two anomeric protons at 5.05 and 5.09 ppm. It is noteworthy that the set of signals yielding larger integrals (“major” CD) essentially coincides with free, noncomplexed 2,6-DM-β-CD. The second set of CD signals with smaller integrals (“minor” CD) showed signals that were noticeably shifted to higher fields, in particular those of the internal hydrogens of the cavity. The other sets of resonances refer to DCV, where two "major" and one "minor" species could be identified. The two major DCV sets were especially evident for the aromatic protons, where two sets for the phenyl hydrogens and two imidazole H-5 singlets were clearly differentiated (Figure 4, left insert), as well as the methyl groups of the Val side chain (Figure 4, right insert). The third set of DCV protons yielded only signals of low intensity and were not shifted compared to the spectrum of DCV (Figure 4B).

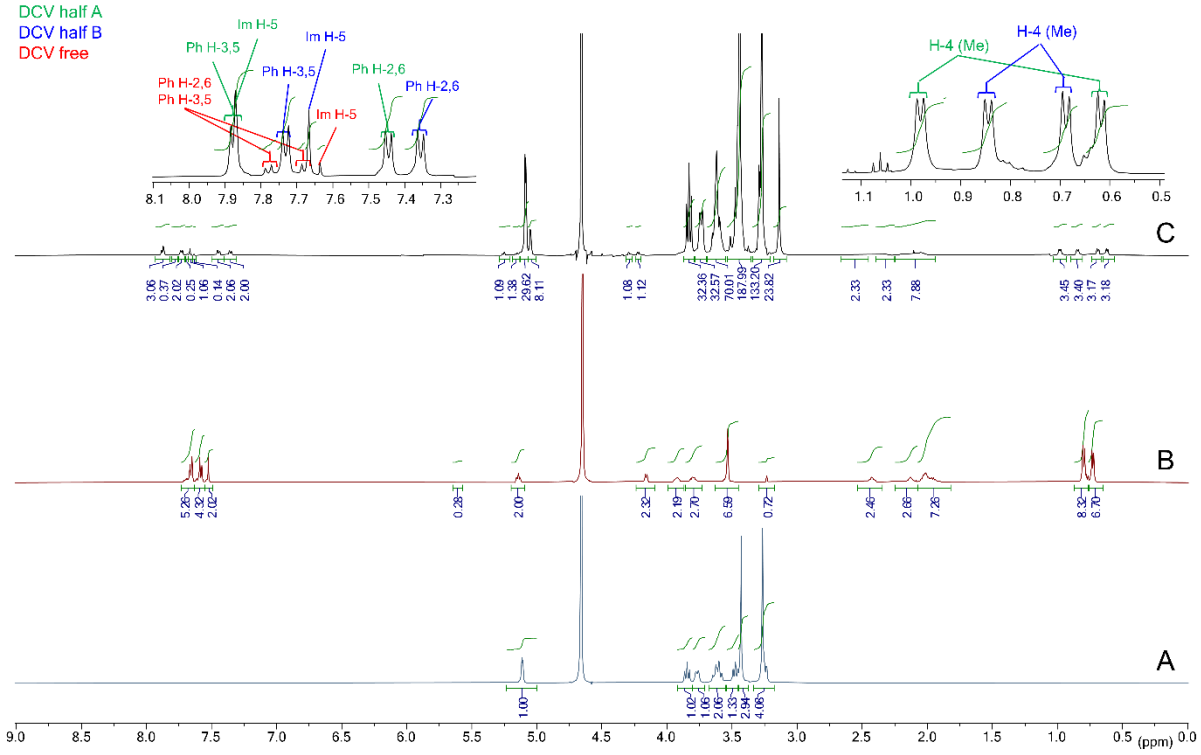

Figure 4 ^{1}H-NMR spectra of (A) 2,6-DM-β-CD, (B) DCV and (C) DCV and 2,6-DM-β-CD in 50 mM deuterated phosphate buffer in D_2O, apparent pH 2.5. The inserts show the expanded region of the aromatic protons (left) and the methyl protons of the Val side chain (right). For signal assignments see Table S1. Experimental conditions: (A) ca. 10 mg 2,6-DM-β-CD in 0.7 mL 50 mM D_3PO_4, in D_2O, pH 2.5; (B) 3.6 mg DCV dihydrochloride in 0.7 mL 50 mM D_3PO_4, in D_2O, pH 2.5; (C) 2.5 mg DCV dihydrochloride and 17 mg 2,6-DM-β-CD in 0.7 mL in 50 mM D_3PO_4, in D_2O, pH 2.5.

The 2D ROESY experiment showed NOE interactions between the signals due to the phenyl protons H-2,6 of both major DCV sets (at 7.44 and 7.35 ppm) and CD protons (Figure S2A). This indicates that these two sets of DCV signals correspond to the two halves of the DCV molecule. Furthermore, the mol:mol ratio between the two main DCV species and the “minor” 2,6-DM-β-CD was 1:1:1 as per comparison of the integrals of selected signals such as the signals of the H-2,6 phenyl protons and the anomeric proton of the D-glucopyranose units. This corresponds to a stoichiometry of DCV:CD of 1:1. Intermolecular NOE interactions involving the aromatic protons of both DCV halves and the internal hydrogens H-3 and H-5 of the minor 2,6-DM-β-CD were also detected (Figure S2A). Furthermore, NOE responses of H-3 and of the 2-OMe group of the CD were stronger with phenyl and the imidazole proton of one DCV species (termed "half A"), while protons of the second DCV species (termed "half B") showed more intense interactions with the H-6 protons as well as the 6-OMe group of 2,6-DM-β-CD. These observations support the formation of an inclusion complex with the diphenyl located inside the CD cavity and the MOC-Val-pyrrolidine moieties protruding from the torus, half A from the wider, secondary side and half B from the narrower primary side of the CD. Intramolecular NOEs involving aromatic hydrogens and protons of the Val side chain methyl groups within each half of the DCV molecule indicate a folded conformation of DCV in the complex. The fact that the ^{1}H-NMR signals of DCV appear as two sets suggests that the DCV molecule within the cavity is constrained in its movement. Typically, only a single set of signals of the solute and another one for the CD are observed in NMR studies of CD complexes (Chankvetadze, 2004; Dodziuk, Koźmiński, & Ejchart 2004; Salgado, & Chankvetadze, 2016; Silva, 2017). An exception was recently noted for the complexation of DCV by γ-CD, where also three sets of signals were observed for DCV as well as the CE (Krait et al., 2020). However, in this case the multiplicity of signals for DCV and γ-CD were due to the simultaneous presence of complexes with 1:1 and 2:1 stoichiometry. The formation of an inclusion complex also rationalizes the shielding of the signals of the H-3 and H-5 protons inside the cavity of 2,6-DM-β-CD due to their proximity to the aromatic rings of DCV so that they were affected by ring current anisotropy. Similar observations were previously made in the previous study involving γ-CD (Krait et al., 2020). No intermolecular NOEs between 2,6-DM-β-CD and the protons of the fifth set of DCV resonances with low intensity were observed. Moreover, these signals were not shifted compared to the DCV spectrum. Thus, this set may tentatively represent free, non-complexed DCV. The ratio was about 0.07:1.0 (free:complexed DCV) as per integrals of the signals at 7.35 and 7.63 ppm indicating that DCV is efficiently complexed by the CD.

Intermolecular NOEs were also noted between the methyl groups of the Val side chain of DCV half A and half B with the internal hydrogens H-3 and H-5 of the major 2,6-DM-β-CD species (Figure S2B).

NOEs with H-3 were more intense than NOEs with H-5. These observations support the formation of higher order complexes with the MOC-Val moieties of DCV entering 2,6-DM-β-CD via the secondary rim. The tentative structure of a complex composed of one DCV molecule and three 2,6-DM-β-CD molecules is shown in Figure 5A. To date, only a few studies have derived higher order complexes between solutes and CDs by NMR measurements (Chankvetadze et al., 2000; Rudzińska, Berlicki, Mucha, & Kafarski, 2007). Due to the large distance to the aromatic rings of DCV, a shift of the resonances of the internal protons of the CDs forming the higher order complex were not noted. Furthermore, the resonances of the side chains of both DCV halves looked identical independent of an interaction. Thus, it cannot be concluded if the higher order complexes have 1:3 stoichiometry (DCV:CD) as shown in Figure 5A or 1:2 stoichiometry with the second CD located either at the "top" or the "bottom" of the initial 1:1 complex.

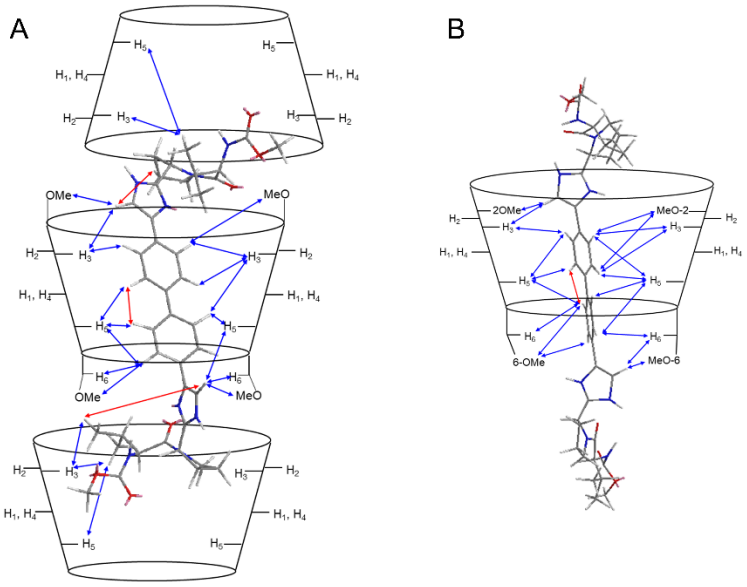

Figure 5 Schematic representation of the structures of the complexes formed between DCV and (A) 2,6-DM-β-CD and (B) TM-β-CD. The intermolecular NOEs derived from ROESY experiments are indicated by arrows: blue, intermolecular NOEs between DCV and the CD; red, intramolecular NOEs.

A DOSY experiment (Figure S3) revealed that the signals corresponding to the major and minor 2,6-DM-β-CD had different diffusion coefficients. Most protons of both halves of DCV displayed approximately the same diffusion coefficients as the minor 2,6-DM-β-CD species, which support the formation of a complex between these molecules. However, no evidence of the interaction between DCV and the major 2,6-DM-β-CD species could be obtained from this experiment. From the present data it cannot be concluded if the complexes with different stoichiometry, i.e., 1:1, 1:2 and/or 1:3, are present simultaneously or if one species dominates. Because no additional signals of either 2,6-DM-β-CD or DCV were observed it may be speculated that the complexes formed by addition of further CD molecules to the 1:1 complex are less stable than the initial 1:1 complex and are formed subsequently. As stated above, typically only a single set of signals of the CD and one for the solute are observed in

NMR studies of CD complexes (Chankvetadze, 2004; Dodziuk, Koźmiński, & Ejchart 2004; Salgado, & Chankvetadze, 2016; Silva, 2017).

The ^{1}H-NMR spectrum of a mixture of *RRRR*-DCV and 2,6-DM-β-CD was also registered (for details see supplementary material) and was almost identical to the spectrum with DCV so that comparable complexes appear to be present including higher order complexes with 1:3 and/or 1:2 stoichiometry. Minor differences were observed for the signals of the Val side chain. These were better resolved in the case of DCV compared to *RRRR*-DCV. Moreover, the NOEs between these protons and the H-3 and H-5 protons of the major 2,6-DM-β-CD species were somewhat less intense for *RRRR*-DCV than DCV. Comparison of the integrals of the set of signals representing the minor and major *RRRR*-DCV revealed a ratio of about 0.14:1.0 (free:complexed DCV, integrals at 7.38 and 7.61 ppm), i.e. approximately twice as much tentatively non-complexed species in case of *RRRR*-DCV. This may suggest the formation of a weaker complex in case of the *RRRR*-enantiomer, which is in accordance with the EMO observed in CE.

3.2.2 Complex DCV and TM-β-CD

The ^{1}H-NMR spectra of DCV and TM-β-CD as well as their mixture in solution at pH 2.5 are shown in Figure 6, signal assignment can be found in Table S2. Five sets of NMR signals were clearly recognizable. Four of these sets were identified as due to major and minor TM-β-CD species and to half A and half B of DCV, respectively. The latter was derived from the NOE interaction seen in the ROESY spectrum between the resonances of the phenyl protons H-2,6 at 7.63 and 7.57 ppm representing the two halves of the molecule. Signals of the major TM-β-CD were identical to the spectrum of TM-β-CD (Figure 6A), while most signals of the minor CD species were shifted upfield as observed for 2,6-DM-β-CD. This indicated inclusion of the biphenyl moiety into the cavity of TM-β-CD. An inclusion complex was further corroborated by NOE interactions of aromatic protons of both DCV halves with the interior H-3 and H-5 protons of the minor TM-β-CD species (Figure S4). An intermolecular NOE interaction involving the 6-OMe group of minor TM-β-CD and the aromatic hydrogens of half B of DCV indicated the proximity of this half of the DCV molecule to the narrower, primary rim of TM-β-CD (Figure S4B). From the NOE data and the fact that the DCV signals appeared as two well-defined sets, it may be concluded that the movement of DCV inside the cavity of the CD is restricted. NOE interactions between the methyl groups of the Val side chain and protons of the major TM-β-CD species were not observed so that there were no indications of the formation of higher order complexes. Therefore, only a complex with 1:1 stoichiometry appears to be present in solution at pH 2.5.

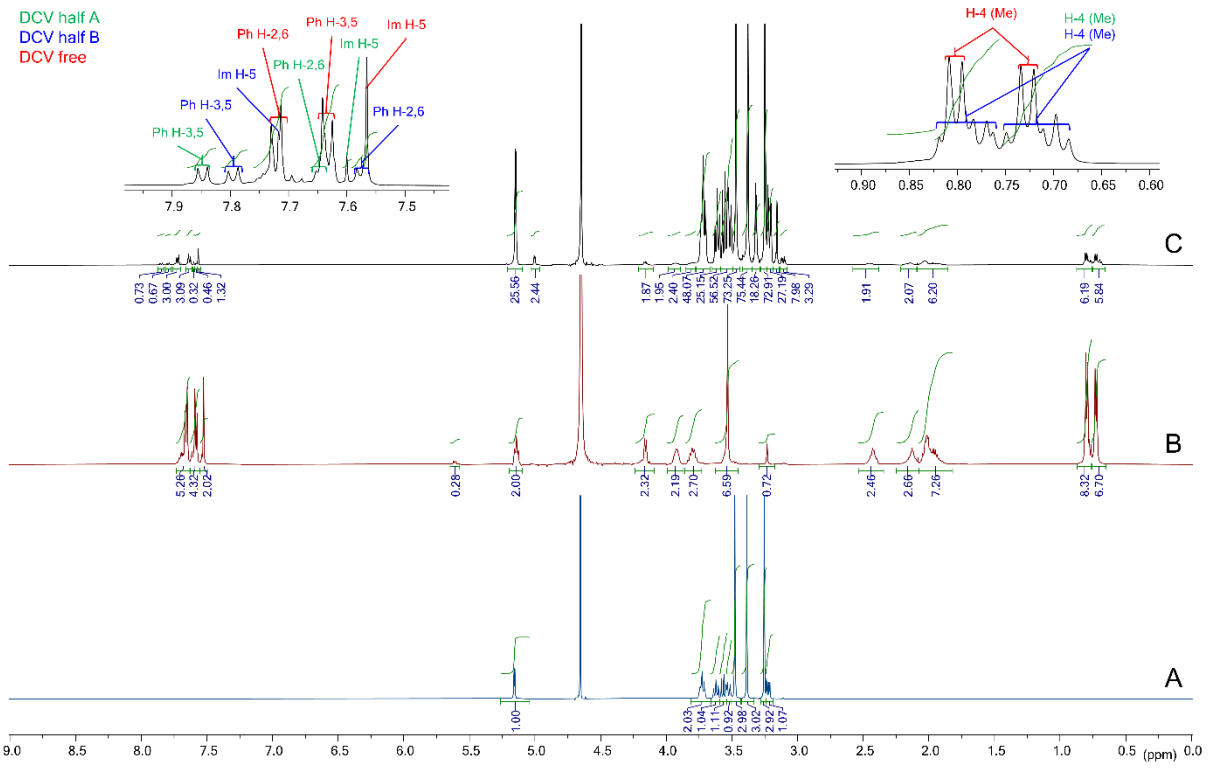

Figure 6 ^{1}H-NMR spectra of (A) TM-β-CD, (B) DCV and (C) DCV and TM-β-CD in 50 mM deuterated phosphate buffer in D_2O, apparent pH 2.5. The inserts show the expanded region of the aromatic protons (left) and the methyl protons of the Val side chain (right). For signal assignments see Table S1. Experimental conditions: (A) ca. 9 mg TM-β-CD in 0.7 mL 50 mM D_3PO_4, in D_2O, pH 2.5; (B) 3.6 mg DCV dihydrochloride in 0.7 mL 50 mM D_3PO_4, in D_2O, pH 2.5; (C) 2.7 mg DCV dihydrochloride and 16.1 mg 2,6-DM-β-CD in 0.7 mL in 50 mM D_3PO_4, in D_2O, pH 2.5.

As in other samples investigated in this study, a fifth set of signals, tentatively assigned to free DCV, was also seen in the ^{1}H-NMR spectrum. In contrast to the spectra of the mixtures containing 2,6-DM-β-CD (or β-CD and 2-M-β-CD, see supplementary material) where higher order complexes appeared to be present, their intensity relative to the signals representing complexed DCV was much higher based on the integrals of the respective signals. A ratio of about 2:1 (free:complexed DCV) was concluded from the integrals at 7.60 and 7.73 ppm. Thus, the amount of non-complexed analytes exceeds the amount of complexed DCV. It may be speculated that the complexation of DCV by TM-β-CD is not that favored and that larger amounts of DCV remained free in solution. Nonetheless, once formed the complex appeared to be dynamically restricted with regard to movement of DCV inside the cavity. In contrast to the CDs yielding an enantioseparation in CD, i.e., 2,6-DM-β-CD, 2-M-β-CD and β-CD, only 1:1 complexes could be concluded from the NMR data. A schematic structure of the complex is shown in Figure 5B.

As in the case of 2,6-DM-β-CD, substantial differences of the complexes of TM-β-CD with the enantiomers DCV and RRRR-DCV were not observed (for a discussion of the ^{1}H-NMR-derived structure of the complex of *RRRR*-DCV see supplementary material). Surprisingly, the ratio between complexed and non-complexed *RRRR*-DCV was opposite to the one observed for DCV, i.e., about 0.58:1.0

(free:complexed) indicating that the complexation of *RRRR*-DCV is favored compared to DCV. Nonetheless, an enantioseparation could not be observed in CE. Whether this is due to a lack of chiral recognition or a consequence of the restricted dynamics (i.e., the slow exchange between free and complexed analyte resulting in the plateau) cannot be derived from the present data.

3.2.3 Complexes DCV and β-CD, 2-M-β-CD, 3-M-β-CD, 6-M-β-CD and 2,3-DM-β-CD

The structures of the complexes of DCV with native β-CD, the methylated derivatives 2-M-β-CD, 3-M-β-CD and 6-M-β-CD as well as 2,3-DM-β-CD were derived from ^{1}H-NMR data as described for 2,6-DM-β-CD and TM-β-CD above. The complexes of the *RRRR*-enantiomer were not studied with these CDs. The results are summarized in Table 1, details of the structure elucidation are described in the supplementary material. In all cases, the two "halves" of DCV could be clearly differentiated, indicating that movement of DCV in the cavity of all CDs is restricted. β-CD, 2-M-β-CD and 6-M-β-CD appeared to form higher order complexes as observed for 2,6-DM-β-CD, based on NOE interactions between the methyl groups of the Val side chain and H-3 and H-5 of the respective major CD species. In contrast, in the case of 3-M-β-CD and 2,3-DM-β-CD, complexes with 1:1 stoichiometry were derived from the data as observed for TM-β-CD. Thus, it may be speculated that upon methylation of the 3-hydroxy groups of β-CD the formation of higher order complexes with DCV is hindered although the structural basis of this phenomenon is not apparent. NMR data did not reveal a significant difference of the conformation of DCV in the complexes because a folded conformation was derived in all cases.

Table 1 CE behavior, stoichiometry and structure of DCV methylated β-CD complexes

CD	CE analysis	Complex stoichiometry	Ratio DCV free:complexed	Comments
β-CD	Enantioseparation	1:3[a]	0.10:1.00	Diphenyl moiety in cavity of 1st CD molecule, MOC-Val moieties included in further CDs
2-M-β-CD	Enantioseparation	1:3[a]	0.06:1.00	Diphenyl moiety in cavity of 1st CD molecule, MOC-Val moieties included in further CDs,
3-M-β-CD	Broad peak	1:1	0.18:1.00	Diphenyl moiety in cavity of CD
6-M-β-CD	Broad peak	1:3[a]	0.08:1.00	Diphenyl moiety in cavity of 1st CD molecule, MOC-Val moieties included in further CDs,
2,6-DM-β-CD	Enantioseparation	1:3[a]	0.07:1.00 0.14:1.00 (*RRRR*-DCV)	Diphenyl moiety in cavity of 1st CD molecule, MOC-Val moieties included in further CDs, DCV in folded conformation, no significant differences between complexes of DCV and *RRRR*-DCV
2,3-DM-β-CD	Plateau	1:1	0.54:1.00	Diphenyl moiety in cavity of CD,
TM-β-CD	Plateau	1:1	2.09:1.00 0.58:1.00 (*RRRR*-DCV)	Diphenyl moiety in cavity of CD, no significant differences between complexes of DCV and *RRRR*-DCV

[a] 1:2 complexes cannot be excluded.

It is interesting to note that the CDs showing enantioresolution in CE at pH 2.5, i.e., 2,6-DM-β-CD, 2-M-β-CD and β-CD form higher order complexes. However, NMR data did not allow to conclude whether 1:1 complexes and the higher order complexes are present simultaneously in solution or if exclusively higher order complexes are formed. Moreover, the data did also not allow to derive the exact

stoichiometry of the higher order complexes, i.e., if 1:3 or 1:2 complexes are present. TM-β-CD and 2,3-DM-β-CD showing the plateau phenomenon seemed to form only 1:1 complexes with DCV. NMR data did not allow to draw conclusions on the strength of the complexes, which might be the cause of the plateau observed in CE. In case of CDs that did not yield an enantioseparation or a plateau but only a broad peak, a 1:1 complex was derived for 3-M-β-CD, while higher order complexes were concluded for 6-M-β-CD. Thus, the CE behavior cannot be predicted from the stoichiometry of the DCV-CD complexes involved.

It is also interesting to note that in case of 2,3-DM-β-CD and TM-β-CD a relatively large amount of DCV seems to exist in the mixtures in the non-complexed state compared to the other CDs. The molar ratio of DCV:CD was not identical in all cases and varied between 1:3 and 1:4, but allowed qualitative conclusions, nonetheless. Thus, about 1/3 to 2/3 of DCV was in the free state in the presence of 2,3-DM-β-CD and TM-β-CD, while this amount ranged between 6 and 15% for the other CDs. It may be speculated, that complete methylation of the secondary rim hinders inclusion complexation of DCV, but once formed, the dissociation of the complex is hampered resulting in a slow equilibrium as the reason for the plateau.

When drawing conclusions on CE separations from NMR studies one has to keep in mind that parameters such as BGE composition and pH can be mimicked in NMR experiments, but especially the concentrations of the CDs and the analytes as well as their ratio differs between the techniques. NMR requires one to two orders higher concentrations of the analytes compared to CE. This implies that information from NMR-derived structures as the basis for the interpretation of CE results has to be considered with care. Nonetheless, such information is valuable in rationalizing CE enantioseparations as shown in many examples (Salgado & Chankvetadze, 2016).

CDs are known to be prone to acid hydrolysis (Szjetli & Budai, 1976), which is acid-catalyzed and temperature-dependent. Although stability of the CDs was not investigated, there were no indication of a significant degradation of the CDs. For example, recording NMR spectra at 25 °C before and after heating the solutions to 80 °C yielded identical spectra and no additional signals could be observed (data not shown). Moreover, identical CE results were observed for freshly prepared BGEs and those kept at room temperature for several hours (data not shown). Thus, it can be assumed that the proton concentration in 50 mM phosphate buffer, pH 2.5, is not high enough to result in a measurable degradation of the CDs, which could affect the presented data.

3.3 Mass spectrometry

Soft-ionization mass spectrometry techniques have also been useful to assess CD complexes (Silion et al., 2021). Electrospray ionization-time of flight-mass spectrometry (ESI-TOF-MS) confirmed the presence of higher order complexes for DCV and 2,6-DM-β-CD (Figure 7A). The signal at *m*/*z* 1035.9883 represents the doubly charged 1:1 complex, while the ions at *m*/*z* 1701.2766 and *m*/*z* 2366.0589 correspond to the doubly charged 1:2 and 1:3 complexes, respectively (for calculated and observed masses, see Table S3). In contrast, essentially only the 1:1 complex was detected at *m*/*z* 1085.0549 when analyzing a solution containing DCV and TM-β-CD (Figure 7B). The most intense signal was due to non-complexed TM-β-CD. The signals of higher order complexes were detected only with a 1000- to 1500-fold lower intensity than the 1:1 complex in the ESI-TOF-mass spectrum (data not

shown). The mass spectrum of the mixture of DCV and β-CD was also recorded for comparison (Figure 7C) because this CD also formed higher order complexes and resulted in an enantioseparation in CE, albeit an approximately 10-fold higher concentration was required. The most intense signal at *m*/*z* 739.3942 refers to non-complexed DCV, while the doubly charged 1:1 complex was detected at a much lower intensity at *m*/*z* 937.3804. The doubly charged ions of the 1:2 and 1:3 complexes could be detected but with a 15- to 200-fold lower intensity (data not shown). Although the MS data of the three CDs cannot be directly compared due to differences in the ionization efficiency of the CDs and their complexes, it may be concluded nonetheless that higher order complexes are readily formed between DCV and 2,6-DM-β-CD, while they do not play a significant role in case of TM-β-CD as previously shown by NMR spectroscopy. Moreover, the 2,6-DM-β-CD complexes appear to be present in higher abundance than the TM-β-CD complex. This is also in accordance with the NMR data where only a low amount of DCV appeared to be non-complexed in contrast to the situation in the presence of TM-β-CD. The relatively low abundance of the ion representing the complex(es) between DCV and β-CD are paralleled by the relatively high concentrations of the CD required in the BGE to obtain an enantioseparation in CE.

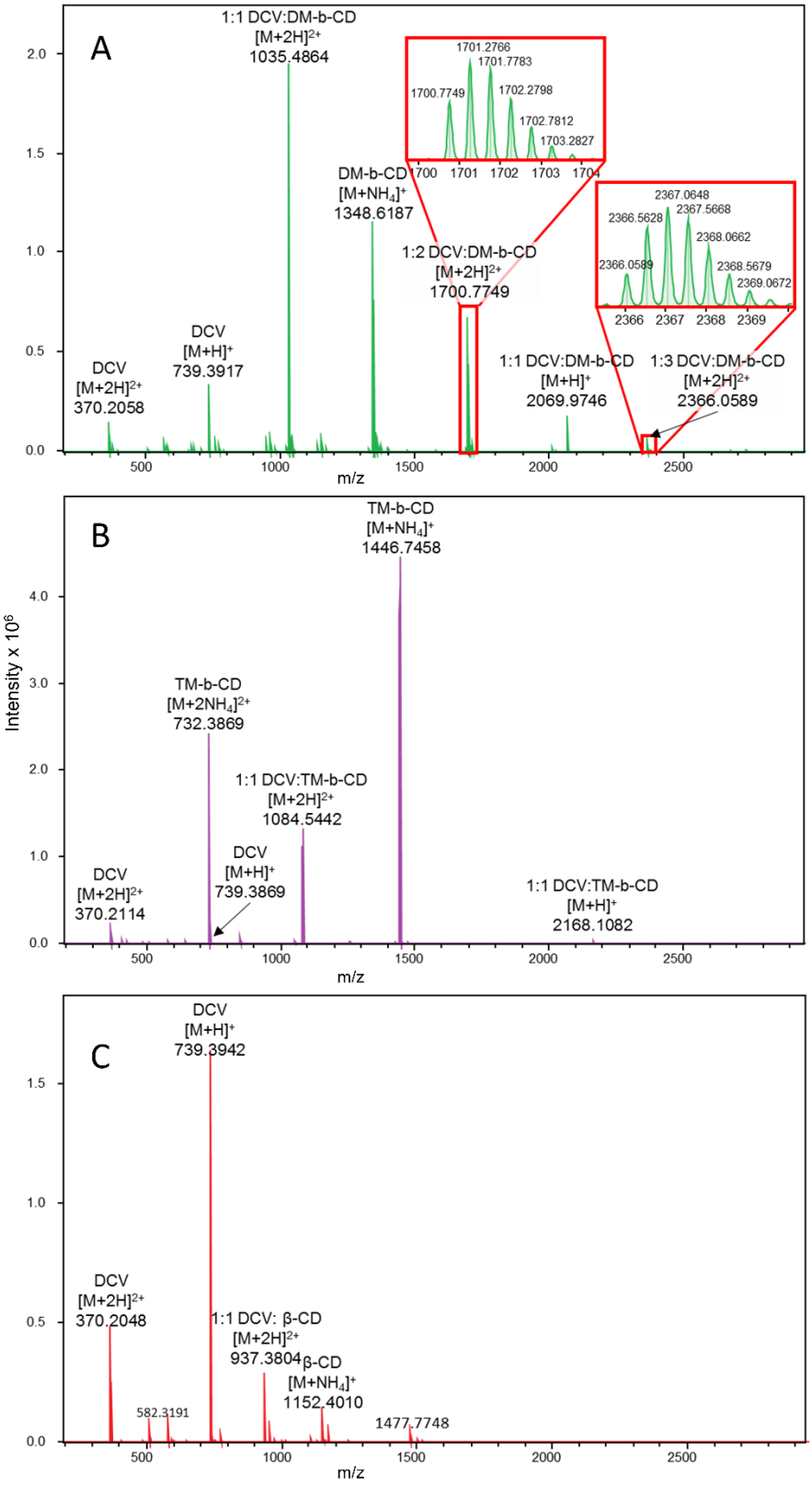

Figure 7 ESI-TOF-mass spectra of solutions of DCV and (A) 2,6-DM-β-CD, (B) TM-β-CD and (C) β-CD in 100 mM ammonium formate buffer, pH 2.6.

4. Conclusions

NMR and mass spectrometry studies have been performed in an attempt to rationalize migration phenomena observed in CE for the enantioseparation of DCV mediated by methylated β-CD derivatives.

Enantioseparations were observed in the presence of 2,6-DM-β-CD and 2-M-β-CD as well as native β-CD, while a broad peak resulted for 6-M-β-CD and 3-M-β-CD. Two peaks with a plateau in between were detected in the case of CDs, featuring a fully methylated secondary rim, i.e., 2,3-DM-β-CD and TM-β-CD. The latter phenomenon was also observed when enantiopure DCV was analyzed. As derived from experiments injecting plugs of CDs and analyte, the presence of the plateau does not represent an enantioseparation but rather a slow equilibrium between DCV and the DCV–CD complex. NMR experiments including ROESY indicated the formation of inclusion complexes in case of all CDs with the diphenyl moiety inside the cavity and the MOC-Val moieties protruding via the primary and secondary opening of the torus. Complex stoichiometry was affected by the substitution pattern. In case of 3-methylated CDs, i.e., 3-M-β-CD, 2,3-DM-β-CD and TM-β-CD, only complexes with a 1:1 stoichiometry could be derived from the NMR data, but all other CDs appeared to form higher order complexes, most likely with a ratio of 1:3 with the MOC-Val residues entering the additional CDs via the secondary rim. The hypothesis, whether the CE behavior of DCV is caused by different complex structures could be only partially confirmed. Thus, the different complex stoichiometries cannot be regarded as the sole reason for the different effects seen in CE. Formation of a 1:1 complex does not automatically imply the occurrence of a plateau as 3-M-β-CD only yields a broad peak. Likewise, higher order complexes do not necessarily result in an enantioseparation, as can be derived from 6-M-β-CD. The ESI-TOF-MS data supported NMR results. In the case of 2,6-DM-β-CD higher order complexes could be observed, while especially for TM-β-CD only very low intensities of the signals of such complexes were detected. Thus, also speculative, it may be concluded that complex formation is somewhat hindered in case of CDs with a "fully methylated" secondary rim. However, once a complex is formed its dissociation could be hampered releasing DCV slowly on the CE timescale, which results in the plateau between the peaks observed in CE.

Conflict of Interest

The authors have declared no conflict of interest.

Acknowledgements

The authors gratefully acknowledge Mylan Laboratories Ltd. (Hyderabad, India) for DCV and Laurus Labs Ltd. (Hyderabad, India) for *RRRR*-DCV. B. C. thanks the Shota Rustaveli National Science Foundation (RNSF) of Georgia (Project No. 217642) for a partial support of this project.

References

Belema, M., van Nguyen, N., Bachand, C., Deon, D. H., Goodrich, J. T., James, C. A., Lavoie, R., Lopez, O. D., Martel, A., Romine, J. L., Ruediger, E. H., Snyder, L. B., St. Laurent, D. R., Yang, F., Zhu, J., Wong, H. S., Langley, D. R., Adams, S. P., Cantor, G. H., Chimalakonda, A., Fura, A., Johnson, B. M., Knipe, J. O., Parker, D. D., Santone, K. S., Fridell, R. A., Lemm, J. A., O'Boyle, D. R., Colonno, R J., Gao, M., Meanwell, N. A., Hamann, L. G. (2014). Hepatitis C virus NS5A replication complex inhibitors: the discovery of daclatasvir. *Journal of Medicinal Chemistry*, 57, 2013-2032. https://doi.org/10.1021/jm401836p.

Bernardo-Bermejo, S., Sánchez-López, E., Castro-Puyana, M., Marina, M. L. (2020). Chiral capillary electrophoresis. *Trends in Analytical Chemistry*, 124, 115807. https://doi.org/10.1016/j.trac.2020.115807

Chankvetadze, B. (2004). Combined approach using capillary electrophoresis and NMR spectroscopy for an understanding of enantioselective recognition mechanisms by cyclodextrins. *Chemical Society Reviews*, 33, 337-347. https://doi.org/10.1039/b111412n.

Chankvetadze, B. (2018). Contemporary theory of enantioseparations in capillary electrophoresis. *Journal of Chromatography A*, 1567, 2-25. https://doi.org/10.1016/j.chroma.2018.07.041.

Chankvetadze, B., Burjanadze, N., Pintore, G., Bergenthal, D., Bergander, K., Mülhenbrock, C., Breitkreuz, J., Blaschke, G. (2000). Separation of brompheniramine enantiomers by capillary electrophoresis and study of chiral recognition mechanisms of cyclodextrins using NMR-spectroscopy, UV spectrometry, electrospray ionization mass spectrometry and X-ray crystallography. *Journal of Chromatography A*, 875, 471-484. https://doi.org/10.1016/S0021-9673(00)00153-9

Dodziuk, H., Koźmiński, W., Ejchart, A. (2004). NMR studies of chiral recognition by cyclodextrins. *Chirality*, 16, 90105. https://doi.org/10.1002/chir.10304.

Fanali, S., B. Chankvetadze, B. (2019). Some thoughts about enantioseparations in capillary electrophoresis. *Electrophoresis*, 40, 2420-2437. https://doi.org/10.1002/elps.201900144

Fejös, I., Kalydi, E., Malanga, M., Benkovics, G., Beni, S. (2020). Single isomer cyclodextrins as chiral selectors in capillary electrophoresis. *Journal of Chromatography A*, 1627, 461375. https://doi.org/10.1016/j.chroma.2020.461375

Guo, C., Xiao, Y. (2021). Negatively charged cyclodextrins: Synthesis and applications in chiral analysis – a review. *Carbohydrate Polymers*, 256, 117517. https://doi.org/10.1016/j.carbpol.2020.117517

Jáč, P., Scriba, G. K. E. (2013). Recent advances in electrodriven enantioseparations. *Journal of Separation Science, 36*, 52-74. https://doi.org/10.1002/jssc.201200836

Krait, S., Salgado, A., Villani, C., Naumann, L., Neusüß, C., Chankvetadze, B., Scriba, G. K. E. (2020). Unusual Complexation Behavior between Daclatasvir and γ-Cyclodextrin. A Multiplatform Study. *Journal of Chromatography A*, 1628, 461448. https://doi.org/10.1016/j.chroma.2020.461448

Pawlotsky, J.-M., Negro, F., Aghemo, A., Berenguer, M., Dalgard, O., Dusheiko, G., Marra, F., Puoti, M., Wedemeyer, H. (2018). EASL Recommendations on Treatment of Hepatitis C 2018. *Journal of Hepatology*, 69, 461–511. https://doi.org/10.1016/j.jhep.2018.03.026

Rudzińska, E., Berlicki, L., Mucha, A., Kafarski, P. (2007). Analysis of pD-dependent complexation of N-benzyloxycarbonylaminophosphonic acids by α-cyclodextrin. Enantiodifferentiation of phosphonic acid pKa values. *Chirality*, 19, 764-768. https://doi.org/10.1002/chir.20450

Salgado, A., Chankvetadze, B. (2016). Applications of nuclear magnetic resonance spectroscopy for the understanding of enantiomer separation mechanisms in capillary electrophoresis. *Journal of Chromatography A*, 1467, 95-144. https://doi.org/10.1016/j.chroma.2016.08.060.

526 Silion, M., Fifere, A., Lungoci, A. L., Marangoci, N. L., Ibanescu, S. A., Zonda, R., Rotaru, A., Pinteala,
527 M. (2021). Mass spectrometry as a complementary approach for noncovalently bound complexes
528 based on cyclodextrins. In A. C. Woods, & C. C. Darie (Eds.), *Advancements of Mass*
529 *Spectrometry in Biomedical Research* (pp. 685-701). Heidelberg: Springer Nature.
530 https://doi.org/10.1007/978-3-030-15950-4_41

531 Silva, M. S. (2017). Recent Advances in Multinuclear NMR Spectroscopy for Chiral Recognition of
532 Organic Compounds. *Molecules*, 22, 247. https://doi.org/10.3390/molecules22020247.

533 Szjetli, J., Budai, Z. (1976). Acid hydrolysis of β-cyclodextrin. *Acta Chimica Hungarica*, 91, 73-80.

534 Varga, E., Benkovics, G., Darci, A., Varnai, B., Sohajda, T., Malanga, M., Beni, S. (2019).
535 Comparative analysis of the full set of methylated β-cyclodextrins as chiral selectors in capillary
536 electrophoresis. *Electrophoresis*, 40, 2789-2798. https://doi.org/10.1002/elps.201900134

537 Yu, R. B., Quirino, J. P. (2019). Chiral selectors in capillary electrophoresis: Trends during 2017-2018.
538 *Molecules*, 24, 1135. https://doi.org/10.3390/molecules24061135

539 Zhu, Q., Scriba, G. K. E. (2016). Advances in the Use of Cyclodextrins as Chiral Selectors in Capillary
540 Electrokinetic Chromatography: Fundamentals and Applications. *Chromatographia*, 79, 1403-
541 1435. https://doi.org/10.1007/s10337-016-3167-0.